RSC Advances

This is an *Accepted Manuscript*, which has been through the Royal Society of Chemistry peer review process and has been accepted for publication.

Accepted Manuscripts are published online shortly after acceptance, before technical editing, formatting and proof reading. Using this free service, authors can make their results available to the community, in citable form, before we publish the edited article. This *Accepted Manuscript* will be replaced by the edited, formatted and paginated article as soon as this is available.

You can find more information about *Accepted Manuscripts* in the Information for Authors.

Please note that technical editing may introduce minor changes to the text and/or graphics, which may alter content. The journal's standard Terms & Conditions and the Ethical guidelines still apply. In no event shall the Royal Society of Chemistry be held responsible for any errors or omissions in this *Accepted Manuscript* or any consequences arising from the use of any information it contains.

ROYAL SOCIETY OF CHEMISTRY

www.rsc.org/advances

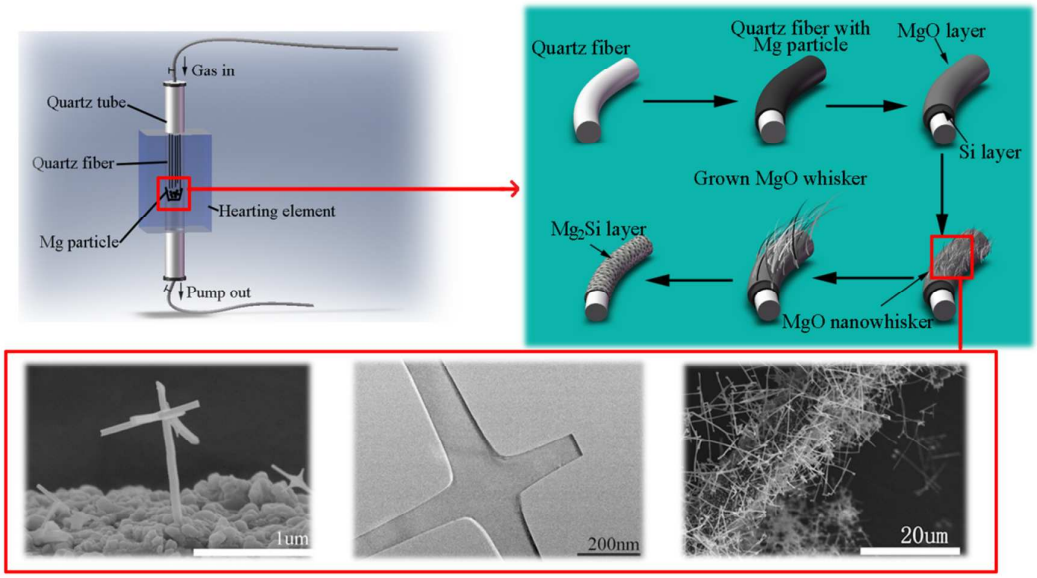

Highlight:

Morphology-controlled MgO Nanowhiskers and "Nanocrosses were prepared on quartz glass fibers by magnesiothermic synthesis at 550°C.

RSC Advances Accepted Manuscript

RSC Advances

Fabrication of Morphology-controlled MgO Nanowhiskers and "Nanocrosses" by magnesiothermic synthesis in vapor phase at 550°C

Yuanjie Mao[1], Minghao Fang[1]*,Zhaohui Huang[1], Haitao Liu[1], Shuyue Liu[1], Yan-gai Liu[1], Xiaowen Wu[1], Xin Min[1], Chao Tang[1], Hao Tang[1], Hui Wu[2]

1. Beijing Key Laboratory of Materials Utilization of Nonmetallic Minerals and Solid Wastes, National Laboratory of Mineral Materials, School of Materials Science and Technology, China University of Geosciences, Beijing, 100083
2. School of Materials, Tsinghua University, Beijing, 100084

Received (in XXX, XXX) Xth XXXXXXXXX 20XX, Accepted Xth XXXXXXXXX 20XX
DOI: 10.1039/x0xx00000x

Morphology-controlled magnesium oxide nanowhiskers have been fabricated on quartz glass fiber substrates using Mg particles as the raw material at relatively low temperatures of 550°C and 600°C. The as-prepared nanowhisker and nanocrosses samples were characterized using Field Emission Scanning Electron Microscopy (FE-SEM), Transmission Electron Microscopy (TEM), Selected Area Electron Diffraction (SAED) and Energy Dispersive X-ray Spectrum (EDS). The MgO nanowhiskers were found to have crystallized structure with growth along the [100] direction. The surfaces of the crossing whisker are considered to be in the (200) lattice plane. The partial pressure of the Mg vapor and the annealing time have played significant roles in determining the diameter and morphology of the nanowhisker. Their adsorption capacity can reduce the concentration of methylene blue solution, which may drive potential applications in biological or environmental areas.

Introduction

One-dimensional (1-D) metal oxide nanostructures (nanowhiskers, nanotubes, nanobelts, etc.) have recently become the subject of great attention and are actively being investigated due to their unique properties in magnetism, catalysis, photocatalysis, adsorption, water disinfection, electro-optical devices, and other potential applications.[1-3] Amongst the 1D oxide materials, magnesium oxide (MgO) is an exceptionally important material in refractory additives, catalysts, antibacterial material, sensors, photonic devices, and as substrates for thin film growth.[4-7] As such, the availability of 1D MgO nano-materials has increased due to the many different methods from different reactants. K.P. Kalyanikutty et al. synthesized MgO nanowhiskers with diameter of 150 nm using a magnesia reduction with carbon as the source of magnesium in the chemical vapor deposition route and at a temperature of 1300 °C.[8]. Youguo Yan et al. reduced the processing temperature to 950 °C by adding Sn as a catalyst reagent.[9] Chengchun Tang et al. reported the synthesis of MgO nanowhiskers with 20nm diameter using Mg and B_2O_3 as the source material at 850 °C.[10] G. Kim et al. observed the formation of a MgO nanowhisker array with diameter of 20-30 nm using Mg_3N_2 as the source material at 950 °C.[11] This large variety of raw materials requires a relatively high decomposition temperature. To solve this problem, Kazuki Nagashima et al. produced a compound MgO nanowire array via pulsed laser deposition.[12] Xiaoxue Zhang et al. reported the synthesis of MgO whiskers via a hydrothermal reaction with graphite oxide held at 120°C for 12 hours.[13] Y. F. Lai et al. prepared magnesium oxide nanowires using $Mg(tmhd)_2$ by pulsed metal organic liquid-injection.[14] Most of these methods require a complex reaction process or the use of expensive raw materials.

In this research, we report on a simple synthesis method for Morphology-controlled MgO nanowhiskers on the surface of a quartz glass fibre. This method uses pure Mg particles as the source material using a magnesiothermic synthesis in the vapor phase at a temperature between 550 °C - 600 °C.

Previous research has explored MgO's adsorption capacity in order to remove toxic metal ions[15], organic pollutants[16, 17] and organic dyes[18, 19]. In this study we test MgO nanowhisker's adsorption capacity with a methylene blue solution. Magnesium oxide is a biodegradable material and researchers have used MgO nanomaterials in the field of medical treatment[20]. Its degradation into magnesium (an essential element of human body) means it may have applications as a drug carrier, biological supporting material or environmental material.

Experimental

RSC Advances Accepted Manuscript

This journal is © The Royal Society of Chemistry 2015

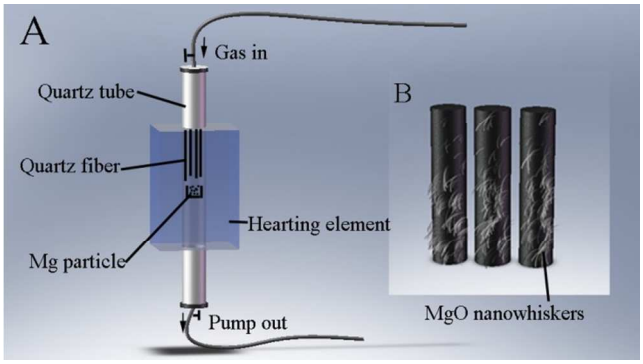

Figure 1 A Schematic of the experimental apparatus used for synthesis of Morphology-controlled MgO nanowhiskers and nanocrosses on a quartz glass fibre. Mg was used as the source material due to a gradient in supersaturation. B: MgO nanowhiskers on a quartz glass fibre that can grow in different conditions in which the products may have different morphology.

The synthesis of MgO nanowhiskers was carried out in a vertical tube furnace. As shown in Figure 1, excess Mg powder was placed in a stainless steel crucible and a bunch of quartz glass fiber was hung from the top of the tube to the upper part of the Mg particle. A mechanical pump was used to pump and flush the quartz tube with Ar three times. The enclosed system was heated in a quartz tube at a temperature between 550 ^{o}C - 600 ^{o}C (5 ^{o}C/min). The heating lasted for 1 h, 2 h, and 4 h before the furnace started to cool down. After the reaction, a product was found on the bottom of the quartz glass fiber surface.

The nanowhisker morphology was characterized by using field emission scanning electron microscopy FESEM (HITACHI S-4600) coupled with energy dispersive spectroscopy (EDS) at an accelerating voltage of 15 kV. High-resolution transmission electron microscopy (HRTEM, Tecnai-G^2-F30, FEI) coupled with energy dispersive spectroscopy (EDS) was used to evaluate the crystal structure and the composition of the nanowhiskers. Samples for HRTEM were prepared by carrying out ultrasonic dispersion in an ethanol solution. A drop of the sample suspension was then placed upon a carbon-coated copper TEM grid. HRTEM measurements were performed at an accelerating voltage of 300 kV. A group of as-synthesized products were put into a glass tube filled with methylene blue solution (7.5mg/L), and then they were allowed to settle for a period of time without stirring. After this period UV spectrophotometry at the wavelength of 664nm was carried out upon the sample.

Results

It can be seen from Figure 2A that fine nanowhiskers are prepared with different diameters on the surface of the quartz glass fiber. The length of the MgO nanowhiskers can reach up to 30 μm. In Figure 2B, the nanocrosses have been fabricated with three-dimensional branches. The crystal structure of the as-prepared samples was characterized by TEM and EDS. The EDS which is shown with HRTEM in Figure 2C, shows that the samples mainly consist of Mg O and a very small amount of Cu which originates from the copper grid. Further quantitative analysis shows clearly that the atomic ratio of Mg:O is nearly 1:1, which implies the presence of MgO nanowhiskers. The HRTEM image (Figure 2D) reveals that the nanowhisker is a single crystal. The planar spacing along the growth direction is 0.21 nm, which

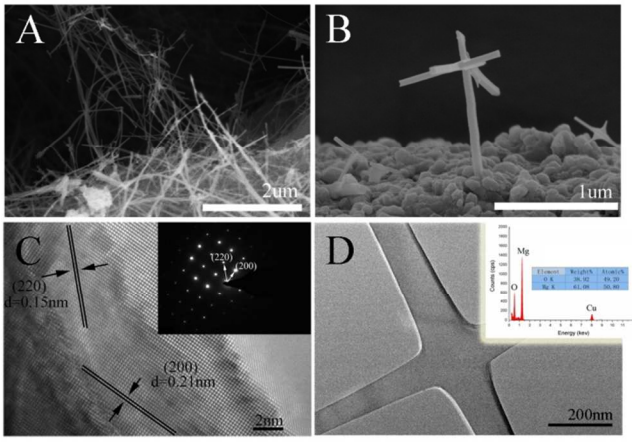

Figure 2. The morphology and the composition of the fabricated single-crystalline nanowhiskers (A: Low-magnification SEM image. B: High-magnification SEM image of the nanocrosses. C: Low-magnification TEM images inset: the EDS spectrum of the nanocrosses. D: HRTEM image and corresponding SAED pattern taken from nanocrosses.)

corresponds to the spacing of the (200) plane in a Mg cubic structure. The selected-area electron diffraction (SAED) that is also shown in Figure 2 confirms this result. The diffraction pattern indicated that the whisker was in the face-centered cubic structure, and the growth direction was determined to be [100].

Figure 3 (A-F) shows how the morphology and whisker diameter varies with heating temperature and time. The diameter of the MgO nanowhisker increases systematically with heating time and goes from 20-30nm (Figure 3A) to 70-100nm (Figure 3C). In Figure 3A-B the MgO keeps its fiber-like morphology whereas in Figure 3C there is a tendency for the MgO to grow into nanocrosses. Samples shown in Figure 3 (A-C) were all grown using the same heating temperature, which means that the partial pressure (42.7 pa) was the same. We can infer that low partial pressures leads to the growth of nanowhiskers and these can mainly maintain the morphology with an extended treating time. However, after long treatment times, the MgO starts to form nanocrosses. Figure 3D and Figure 3E shows that MgO readily forms nanocrosses in 600 ^{o}C, and the diameter can extend further to 250nm. In Figure 3F we can see a coarse substrate surface which results from Si reacting with Mg vapor in order to generate Mg_2Si. However in Figure 3 (D-F) it is shown that in a relative high partial pressure (133 pa), MgO will easily grow into nanocrosses. The diameter of nanocrosses gets larger with extended treatment time and they eventually fall off the quartz glass fiber. We can infer that at higher temperatures MgO tends to grow in all directions forming MgO particles.

When the temperature rises to over 550^{o}C Mg vapor begins to be generated and spreads on the surface of the quartz glass fiber. A reaction takes place between the vapor and the quartz fibre as shown in Figure 4. After further deposition time, Si and MgO layers can be formed upon the quartz glass fibre surface. Supersatuation of Mg vapor then eventually leads to the growth of nanowhiskers. The deposition of Si and MgO layers on the quartz fibre means that Mg that has not had time to react earlier can now react with the trace amount of oxygen contained in the system. Further heating time at 550 ^{o}C leads to the growing of nanowhiskers and formation of branch crystals. Finally, when the heating time is extended even further, Mg_2Si can take the place of

RSC Advances Accepted Manuscript

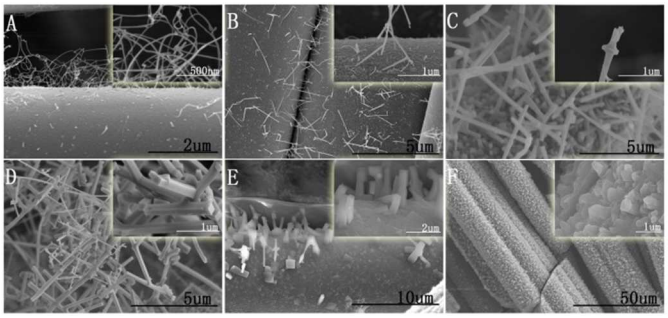

Figure 3. Different morphologies of fabricated MgO nanowhiskers (A: diameter 20-40nm, 550 °C 1 h. B: diameter 50-80nm, 550 °C 2 h. C: diameter 100-150nm, 550 °C 4 h. D: diameter 150-250nm, 600 °C 1 h. E: diameter 150-250nm, 600 °C 2 h. F: coarse surface of substrate fiber, 600 °C 4 h)

the Si layer which means that MgO nanowhiskers can no longer stay in the matrix.

Figure 5 shows the adsorption capacity of the samples fabricated at temperature 550 °C for 2 hours. It is clear that the bundle of fibers with magnesium oxide on the surface exhibit better adsorption capacity than the matrix fibers, which were used as a control group. The data shows that the maximum adsorption capacity was obtained after nearly 10 hours. It can reduce the absorbance from 1.269 to 1.063 in 20ml 7.5mg/L methylene blue solution. The difference in adsorption capacity can be attributed to an increase of surface area. We can estimate of its load capacity on drugs according to its adsorption performance

Discussion

In our experiment, The VS mechanisms are used to explain the growth of whiskers. According to previous research, the VLS model has been used to explain the growth mechanism at high temperatures, while the VS model dominates at low temperatures.[21] In this experiment MgO nanowhiskers were synthesised at a relatively low growth temperature and no droplets were found on top of the nanowhiskers as shown in the SEM and TEM characterizations. This means that the growth of nanowhiskers does not follow the (VLS) growth model.[22, 23] We can infer that the Mg was coming from the heating of Mg particles, and there is direct adsorption of the Mg gas phase onto a solid surface while the presence of O can be attributed to two possible sources. Firstly, it is possible that there is direct diffusion from the quartz glass fiber. Secondly, it is possible there is a small amount of oxygen remaining in the quartz tube. We can infer that during the generation of MgO nanowhiskers, some selected crystal planes are more active compared with other ones. Mg atoms may deposit on these crystal planes and then form single crystal Mg. However, due to the competition of nucleation rates and growth rates in these planes Mg whiskers may have different morphologies. The work of D. A. Grynko et al. confirms this process by comparing different growth mechanisms in CdS nanowires.[24] Mg whiskers can quickly change into MgO whiskers since Mg is oxidized very easily. The size of the produced MgO nanowhiskers can get larger by extending the heating time and temperature. Previous studies agree that Mg vapor concentration in the reaction tube is potentially responsible for the difference in

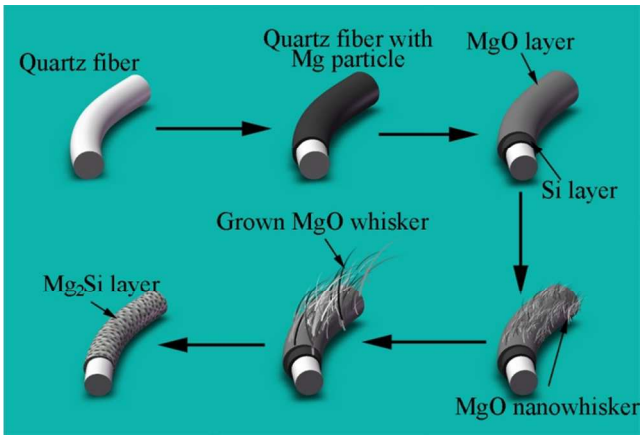

Figure 4. The MgO whisker fabrication process at 550°C

size and growth mechanism of products.[25] In vertical furnaces, Mg vapor can only exist within a limited field distribution according to the concentration in the vertical direction. This is simply due to the low pressure and also due to gravity.

Due to the evaporating of Mg at a high rate, reproducibility may be one of the challenges pure Mg is used as the source material. In this case, by controlling the heating temperature and distance from Mg particles, we can easily control the partial pressure of Mg vapor and make it stay in a particular state in order to get MgO whiskers of different diameters or morphology.

As we can see from Figure 6, the quantity of broken bonds for each plane in each unit cell is seen to be ten for the (111) crystallographic plane, nine for the (200) crystallographic plane and nine for the (220) crystallographic plane. The quantity of broken bonds per unit area for each crystal plane is calculated to be 0.71 $Å^{-2}$ for (220), 0.65 $Å^{-2}$ for (111) and 0.51 $Å^{-2}$ for (200), which means that the surface energies (γ) follow the following trend: γ （200）< γ （111）< γ （220）. Other research indicates that the facet selectivity can be understood by the differences in the surface energies of the different facets.[27] In this case, (200), (020) and (002) planes can easily form surfaces upon a square fiber because of their low surface energies and it is also favorable to serve as a nucleation seed, which can support the further crystal growth by a vapor–solid (VS) mechanism.

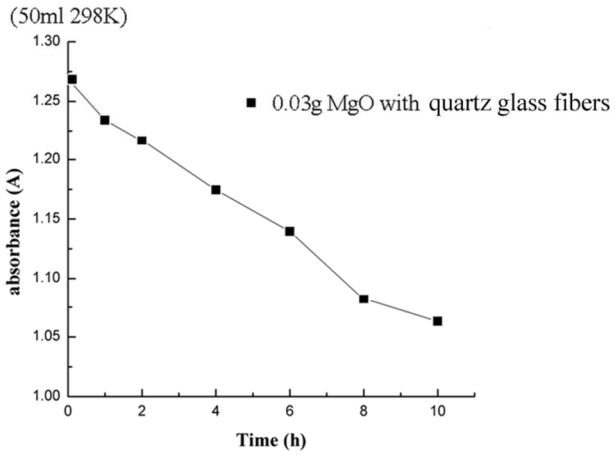

Figure 5. Adsorption capacity of the products fabricated at the temperature of 550 °C for 2 h.

RSC Advances Accepted Manuscript

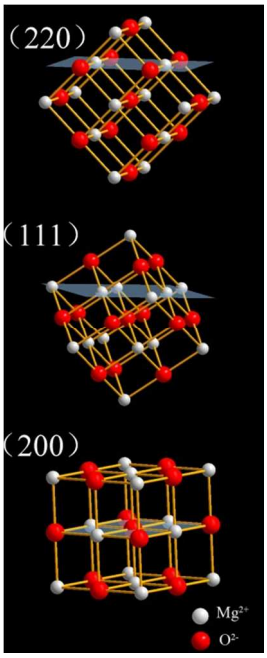

Figure 6 The unit cell model of MgO along [111], [200] and [220] directions obtained from data supplied by ICSD-26958.[26]

Figure 7A shows the formation of a mass three-dimensional branch crystal structure. During the reaction process, Mg vapor first reacts with the quartz glass fiber, which causes a partial reduction in Mg vapor at the surface of the matrix. In this kind of environment, MgO nanowhiskers have a fixed orientation towards the area where Mg vapor concentration is highest until they reach sufficient length. As the whiskers get longer, it produces many crystal branches in an orthogonal direction with a competition of nucleation rates and growth rates in these planes due to symmetry of the cubic structure. The (200), (020), and (002) planes all have equally low surface energies which means the crystal can grow along three different directions without exterior guidance. Figure 7B shows two interesting features. Firstly, on the right-hand-side of the image there is a small embossment, which shows the fresh formation of a branch crystal. Secondly, the black section on the left-hand part of the image is a contrast change due to an out-of-pane branch. As a result of this feature, we can get MgO nanocrosses (Figure 7C) if the ambience is the same in one dimension. This kind of feature can be used to generate specific morphology materials by the control of the direction and concentration of Mg vapor. Such work will be carried out in a future study.

Conclusions

In summary, continuous MgO nanowhiskers with controllable morphology were produced by using Mg vapor in a vertical tube furnace. This approach has allowed the generation of MgO nanowhiskers and nanocrosses in a simple way at relatively low temperatures (550 ^{o}C -600 ^{o}C). The MgO nanowhiskers have controllable diameter from 20nm to 200nm and the crystallographic orientation of the surfaces in the square whisker is along the (200) plane. This is thought to be due to the lower between nucleation and growth rates in different plans. VS is considered to be the main mechanisms for the growth of the

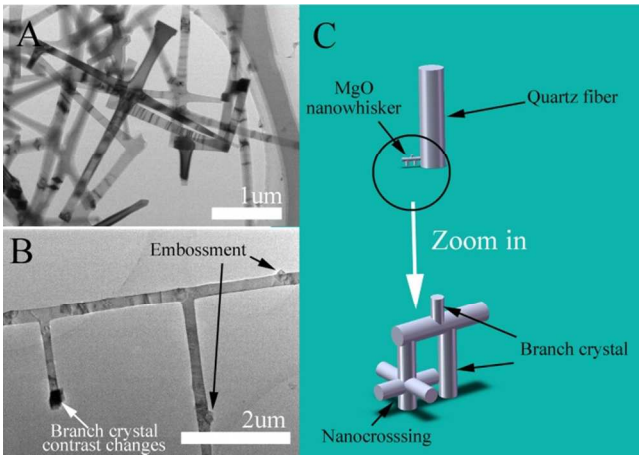

Figure 7. The formation sequence of MgO branch crystala and nanocrossing. (A B:Low-magnification TEM images of nanocrosses C:simulation nanocrosses)

MgO nanowhiskers. Finally, we note that the grown MgO nanowhiskers show excellent adsorption capacity that reach a maximum after 10 hours of exposure. This leads to potential applications in environmental and biological science.

Acknowledgements

This work was financially supported by the National Natural Science Foundation of China (NSFC Grant No.51172216) and the Fundamental Research Funds for the Central Universities for financial support (Grant Nos. 2652013126)

Notes and references

[a]*School of Materials Science and Technology, China University of Geosciences(Beijing), Beijing 100083, P.R.China. Fax: +86 10 82322186; Tel: +86 10 82322186; E-mail: fmh@cugb.edu.cn*

1. J. Liu, O. Margeat, W. Dachraoui, X. Liu, M. Fahlman and J. Ackermann, *Adv. Funct. Mater.*, 2014, **24**, 6029-6037.
2. V. E. Bochenkov and G. B. Sergeev, *Catalysis in Industry*, 2010, **2**, 1-10.
3. C. Liu, X. Xie, W. Zhao, J. Yao, D. Kong, A. B. Boehm and Y. Cui, *Nano Lett.*, 2014, **14**, 5603-5608.
4. F. Al-Hazmi, F. Alnowaiser, A. A. Al-Ghamdi, A. A. Al-Ghamdi, M. M. Aly, R. M. Al-Tuwirqi and F. El-Tantawy, *Superlattices Microstruct.*, 2012, **52**, 200-209.
5. A. A. Al-Ghamdi, F. Al-Hazmi, F. Alnowaiser, R. M. Al-Tuwirqi, A. A. Al-Ghamdi, O. A. Alhartomy, F. El-Tantawy and F. Yakuphanoglu, *J. Electroceram.*, 2012, **29**, 198-203.
6. H. Tan, N. Xu and S. Deng, *Journal of Vacuum Science & Technology B: Microelectronics and Nanometer Structures*, 2010, **28**, C2B20.
7. S. K. Shukla, G. K. Parashar, A. P. Mishra, P. Misra, B. C. Yadav, R. K. Shukla, L. M. Bali and G. C. Dubey, *Sensors Actuators B: Chem.*, 2004, **98**, 5-11.
8. K. P. Kalyanikutty, F. L. Deepak, C. Edem, A. Govindaraj and C. N. R. Rao, *Mater. Res. Bull.*, 2005, **40**, 831-839.
9. Y. Yan, L. Zhou, J. Zhang, H. Zeng, Y. Zhang and L. Zhang, *The Journal of Physical Chemistry C*, 2008, **112**, 10412-10417.
10. C. Tang, Y. Bando and T. Sato, *The Journal of Physical Chemistry B*, 2002, **106**, 7449-7452.
11. G. Kim, R. L. Martens, G. B. Thompson, B. C. Kim and A. Gupta, *J. Appl. Phys.*, 2007, **102**, 104906.
12. K. Nagashima, T. Yanagida, H. Tanaka and T. Kawai, *J. Appl. Phys.*,

RSC Advances Accepted Manuscript

2007, **101**, 124304.
13. X. Zhang, K. Qiu, E. Levänen and Z. X. Guo, *CrystEngComm*, 2014, **16**, 8825.
14. Y. F. Lai, P. Chaudouët, F. Charlot, I. Matko and C. Dubourdieu, *Appl. Phys. Lett.*, 2009, **94**, 022904.
15. C. Y. Cao, J. Qu, F. Wei, H. Liu and W. G. Song, *ACS Appl Mater Interfaces*, 2012, **4**, 4283-4287.
16. L. Lange and S. K. Obendorf, *Arch. Environ. Contam. Toxicol.*, 2012, **62**, 185-194.
17. V. Nagarajan and R. Chandiramouli, *Journal of Inorganic and Organometallic Polymers and Materials*, 2014, **24**, 1038-1047.
18. F. Sánchez-Ochoa, G. H. Cocoletzi, G. I. Canto and N. Takeuchi, *J. Appl. Phys.*, 2014, **115**, 213507.
19. N. K. Nga, P. T. T. Hong, T. D. Lam and T. Q. Huy, *J. Colloid Interface Sci.*, 2013, **398**, 210-216.
20. D.-R. Di, Z.-Z. He, Z.-Q. Sun and J. Liu, *Nanomed. Nanotechnol. Biol. Med.*, 2012, **8**, 1233-1241.
21. S.-Y. Kuo and H.-I. Lin, *Nanoscale Research Letters*, 2014, **9**, 1-5.
22. K. Tai, K. Sun, B. Huang and S. J. Dillon, *Nanotechnology*, 2014, **25**, 145603.
23. T. Yanagida, K. Nagashima, H. Tanaka and T. Kawai, *Appl. Phys. Lett.*, 2007, **91**, 061502.
24. D. A. Grynko, A. N. Fedoryak, O. P. Dimitriev, A. Lin, R. B. Laghumavarapu and D. L. Huffaker, *Surface & Coatings Technology*, 2013, **230**, 234-238.
25. Y. Chen, J. Li, Y. Han, X. Yang and J. Dai, *J. Cryst. Growth*, 2002, **245**, 163-170.
26. W. Gerlach, *Z. Phys.*, 1922, **9**, 184-192.
27. M. S. Hu, W. M. Wang, T. T. Chen, L. S. Hong, C. W. Chen, C. C. Chen, Y. F. Chen, K. H. Chen and L. C. Chen, *Adv. Funct. Mater.*, 2006, **16**, 537-541.

RSC Advances Accepted Manuscript

This journal is © The Royal Society of Chemistry 2015